Hindawi
Advances in Civil Engineering
Volume 2023, Article ID 9960412, 16 pages
https://doi.org/10.1155/2023/9960412

Research Article

Predicting Strength Properties of High-Performance Concrete Modified with Natural Aggregates and Ferroslag under Varied Curing Conditions

Muthumani Soundararajan,[1] Sridhar Jayaprakash,[2] S. K. Maniarasan,[3] and Ravindran Gobinath[4]

[1]*Department of Civil Engineering, Sona College of Technology, Salem, India*
[2]*Department of Civil Engineering, GMR Institute of Technology, Rajam, India*
[3]*Kongu School of Architecture, Perundurai, India*
[4]*Department of Civil Engineering, School of Engineering, SR University, Hyderabad, Telangana, India*

Correspondence should be addressed to Ravindran Gobinath; gobinathdpi@gmail.com

Received 28 September 2022; Revised 28 May 2023; Accepted 6 June 2023; Published 19 June 2023

Academic Editor: Süleyman İpek

High-performance concrete (HPC) is obtained by inclusion of mineral admixtures like silica fumes and fly ash to the normal concrete. Consumption of natural materials such as sand, natural aggregates, and limestone produces environmental degradation. Similarly, industrial by-products such as fly ash, silica fume, and ferro slag need to be safely disposed of without negatively impacting the environment. The problem being addressed in this study is the need to develop high-performance concrete (HPC) that is durable and environmentally friendly. In recent years, the use of natural aggregates and ferro slag as partial replacements for traditional aggregates has gained attention as a sustainable alternative in the production of concrete. However, there is limited research on the effect of these materials on the mechanical and durability properties of HPC under varied curing conditions. In this current research, high-performance concrete of M60 grade with partial substitution of coarse aggregate with ferro slag aggregate was formed as per the recommendations of the American Concrete Institute with the inclusion of fly ash and silica fume. Natural coarse aggregate was partly substituted by ferro slag aggregate in proportions from 0% to 40%. Partial substitution of cement was made with 15% of fly ash and 10% of silica fumes. Specimens of normal concrete mix (MF0) and modified ferro slag aggregate concrete mix (MF20, MF30, and MF40) were prepared and subjected to acid test, sulphate test, and alternate wet and drying tests to assess the compressive strength of the concrete mixes. Central composite design (CCD) of RSM modelling was adopted to recommend a regression model to forecast the compressive strength of concrete under wetting drying test, acid test, and sulphate attack. Further, natural aggregate, ferro slag, and duration of curing were considered as basic variables to suggest the model. Regression models for response data were evaluated using analysis of variance (ANOVA) and Pareto charts. The results show that the mix MF30 (30% substitution of natural aggregate by ferro slag aggregate) had higher compressive strength. The residual compressive strength at 270 days under alternate wetting and drying, acid attack, and sulphate attack was obtained as 62 MPa, 62.50 MPa, and 66.50 MPa, respectively. Similarly, the percentage loss of weight was obtained as 12.92%, 12.22%, and 6.60% for alternate wetting and drying, acid attack, and sulphate attack, respectively. The findings of the analysis of variance (ANOVA) indicate that the most significant factors influencing the variables CS_{WD}, $CS_{AT,}$ and CS_{ST} are natural aggregate, ferro slag, and curing period. The regression models for CS_{WD}, $CS_{AT,}$ and CS_{ST} are extremely significant, as shown by the ANOVA and Pareto chart analyses.

1. Introduction

Concrete is a well-known and a versatile building material in the world. It is widely used in the development and construction of various kinds of infrastructure such as buildings, bridges, and dams. It possesses qualities that are important and noticeable in the field of infrastructure construction, such as strength, durability, convenience of placement, and economy. It is a combination of cement, sand (fine aggregate), crushed stone (coarse aggregate), and water. Along with the advancements in science, engineering, and technology, many kinds of concrete have been developed. However, the production and use of concrete can have significant environmental impacts, including the emission of greenhouse gases, the exhaustion of natural resources, and the generation of waste. To address these environmental issues, researchers have been exploring the development of high-performance concrete (HPC). HPC is a type of concrete that is designed to have superior mechanical and durability properties compared to conventional concrete while also reducing its environmental impact. HPC can be produced with lower amounts of cement, which reduces carbon emissions, and can incorporate recycled materials such as fly ash, slag, or silica fume, reducing waste and conserving natural resources. High-performance concrete (HPC) is concrete that satisfies certain performance and uniformity standards that are often impossible to accomplish using standard ingredients, customary mixing, putting, and curing procedures. Only low w/c, which requires usage of high cement content, may be used to satisfy special performance criteria using standard materials for applications like bridges, windmill towers, utility towers for oil and gas industry, offshore structures, hydraulic structures, and overlay materials. It is characterized by its early high strength, high density, low shrinkage, high modulus of elasticity, and impervious nature [1]. Moreover, it is strongly corrosion-resistant and is durable in acid and alkaline environments. High-performance concrete is compatible with the steel reinforcement embedded in the concrete and thus provides a better bonding. It extends the concrete structure's service life, causes minor damage, and lowers the cost of future repairs of the concrete structure. However, the initial production cost of the HPC is considerably high. The concrete with uniaxial strength under compression is higher than that of the control concrete produced in a given geographical location, which can be regarded as the high-strength concrete. The compressive strength of the concrete cylindrical specimen of 28-day age made up of high-strength concrete will be greater than 42 MPa. Condensed silica and microsphere fly ash improved the packing density, flowability, and strength aspect of the concrete for a low water cement ratio of 0.35 [2]. Ultra-high-performance concrete has outstanding freezing-thawing resistance due to its condensed microstructure. Similarly, usage of steel fibres in UHPC increases the load-carrying capacity [3]. UHPC containing 10% substitution of steel slag shows higher flow capacity when compared to control concrete [4]. Concrete with 10% steel replacement of coarse aggregate with steel slag shows development in compressive strength, whereas no significant development is detected in split tensile strength and flexural strength [5]. UHPC containing 3% of nano-titanium dioxide (TiO_2) and 30% of low-carbon fly ash shows a reduction in strength at the age of 56 days when subjected to chloride diffusion and sulphuric acid [6]. Concrete strength is improved with respect to that of the steel slag aggregate replacement for all mix proportions associated with that of conventional concrete. Similarly, water absorption capacity of steel slag aggregate concrete is more than that of conventional concrete. The presence of the inert lime in the concrete mix caused swelling of the concrete in the longer run [7]. Self-compacting concrete containing steel slag increases the stiffness and brittleness up to 20% replacement, beyond which the strength decreases. The addition of steel slag has an effect on the Poisson ratio of concrete [8]. The fracture performance of concrete increases up to 10% replacement of cement by weight of steel slag powder, beyond which it shows a negative effect. This negative effect may be due to low cementitious activity [9]. High-performance concrete not only satisfies the strength of the concrete but also increases durability of the cement matrix exposed to the environmental effects. The microstructure arrangements of the high-performance concrete provided low porosity and are much less permeable compared to those of the normal concrete [10]. The half-cell potential values obtained through a half-cell potentiometer provide information about corrosion and indicate the areas of corrosion in the steel bar embedded in the concrete. An adequate concrete cover as per the codal provision was more important in reducing the corrosion of rebar in the concrete in the long run [11]. Ferrocement composites having 30% of steel slag as fraction of fine aggregate show increases in initial crack load and failure load and less deflection [12, 13]. Response surface methodology, a statistical and mathematical approach to design of experiments (DOE), can be used to determine the impact of independent factors on results with the fewest number of tests [14–17]. To calculate the compressive strength of concrete, artificial neural networks (ANNs) using three-variable process modelling and response surface methodology (RSM) are both effective techniques [18]. Comparatively speaking, the RSM model's prediction of compressive strength using nondestructive testing has a high degree of accuracy when compared to other models like the power-power model, bilinear model, double exponential model, and logarithmic model [19]. When validated with experimental findings, experiments made for geopolymer concrete utilising the Box–Behnken response surface approach revealed an inaccuracy of 2.24% [20]. Compressive strength of UHPC having GGBS, fly ash, and silica fumes is greater than 120 MPa. All the specimens had goethite-like structures (corrosion by-products) visible at 90 days. Compared to GGBS, the usage of fly ash sped up the synthesis of such compounds [21]. With a flexure strength of 29 MPa and compressive strength of 111 MPa after 28 days, specimens with a content of coarse coal

gasification slag of less than 25% can meet the strength requirements for nonstructural HPC [22]. The mechanical characteristics of HPC were steadily enhanced as a result of the greater polypropylene fibre (PP) content. The superior performance of freshly formed and cured HPC with 46% GGBS in place of cement with 0.025–0.25% PP fibre content demonstrates the wide range of applications for these mixtures [23].

In this study, high-performance concrete of M60 grade was prepared with the addition of fly ash and silica fumes with 15% and 10% replacement by weight of cement. Moreover, coarse aggregate was partially substituted by ferro slag aggregate in different proportions from 0% to 40%. To assess the durability properties of concrete, acid test, sulphate test, and alternate wet and dry tests were conducted at different curing ages. In order to obtain the ideal combination of progression variables (natural aggregate, ferro slag, and curing period) and to develop a regression model for predicting compressive strength under different curing periods, central composite design (CCD)-RSM statistical study was accomplished.

2. Materials

Ordinary Portland cement (OPC) of 53-grade in compliance with IS 12269 (1987) [24] was purchased from a local market and used in the various concrete mixes. Low-calcium fly ash (Class F) with specific gravity of 2.24 was used as a partial replacement for the cement. Silica fume is used for filling the major pores in the concrete, thereby reducing the porosity to a considerable amount, increasing the compactness, and improving the density of the concrete. The chemical composition of silica fume and fly ash is shown in Table 1. The sand used is passed through 4.75 mm IS sieve and conforms to Grading Zone-II of IS 383 [25]. The well-graded granite stone and ferro slag aggregate from steel residue were used as coarse aggregate. Coarse aggregates of 12.5 mm were adopted for all the concrete mixes. The natural stone aggregates were selected conforming to IS 383 [25]. The physical properties of ferro slag aggregate and coarse aggregate are shown in Table 2. A water reducer, CONPLAST SP 430, was used as a chemical admixture, which enhanced the pozzolanic reaction of fly ash. The specific gravity of the fly ash concrete mix was 1.81 with solid content of 26%.

2.1. Concrete Mix Ratio. The mixture of concrete was designed as per ACI Standards 211.4R [26] depending on the M60 grade. The ratio of the water to cement in the concrete mix is 0.48, and the proportion is 1 : 1.40 : 2.32. The quantity of binder content was adopted as 15% for fly ash and 10% for silica fume by weight of cement content. The admixtures, namely, fly ash and silica fume, were added to the concrete mix to realize the desired strength of the concrete. The quantity of ferro slag aggregate was varied on the basis of the 0% to 100% replacement of the natural aggregate. Superplasticizer was added to the concrete mix to obtain a workability of 100 mm for all mixes. The details of the mix are given in Table 3.

Table 1: Chemical composition of silica fumes and fly ash.

Composition	Silica fumes	Fly ash
SiO_2	93.5	59.3
Al_2O_3	0.27	34.6
Fe_2O_3	0.23	5.87
CaO	0.41	1.02
MgO	1.01	0.38
SO_2	0.40	0.1
K_2O	1.51	0.23
Na_2O	0.79	1.54

Table 2: Physical properties of ferro slag aggregate and coarse aggregate.

Description	Ferroslag aggregate	Coarse aggregate
Specific gravity	2.82	2.76
Bulk density	1613.06 kg/m^3	1653.06 kg/m^3
Surface moisture	0.05%	0.086%
Water absorption	0.8%	1.00%
Fineness modulus	7.2	6.98
Impact value	26.5%	25.3%
Crushing value	27.5%	25.5%
Abrasion value	28.1%	26.5%

3. Experimental Investigation

3.1. Optimising the Mix Proportions. The experimental investigation involves such that for each above case mentioned in Table 3, concrete cubes of size 15 cm × 15 cm × 15 cm for M60 grade of the concrete will be investigated for compressive strength. The cast cubes were verified for compressive strength, after three days, seven days, and twenty-eight days of curing as per the recommendations of IS 516 [27]. The strength of compression analysis is made in compression machine with 1000 kN which is tested in a universal testing machine with 1000 kN load cell limit. The optimum mix proportion which has higher compressive strength was selected for further durability studies.

3.2. Durability Studies

3.2.1. Alternate Wet and Dry Testing. An alternate wetting and drying test was performed on the concrete cubes of a standard size of 100 mm × 100 mm × 100 mm. The concrete cube specimens after twenty-eight of curing were exposed to wet and dry tests by placing the cubes in water for 24 h and then air room temperature for 24 h as per the standard test procedures, and this alternate dry and wet test was carried out at different ages. The test procedure as per IS 4332: Part 4 [28] was followed while testing the concrete specimens. The testing procedure was repeated regarding 56 days, 90 days, 120 days, 180 days, and 270 days of alternate wetting and drying of the specimens. The concrete specimen was

Table 3: Concrete mix design proportions.

Mix ID	Cement	Fly ash	Silica fume	Fine aggregates	Coarse aggregates		Water (l/m^3)	Superplasticizer (l/m^3)
				(kg/m^3)	Natural aggregates	Ferro slag aggregates		
MF0	382.5	76.5	51	716.17	1186.56	0.00	143	4.54
MF10	382.5	76.5	51	716.17	1067.90	118.65	143	4.54
MF20	382.5	76.5	51	716.17	949.24	237.31	143	4.54
MF30	382.5	76.5	51	716.17	830.59	355.96	143	4.54
MF40	382.5	76.5	51	716.17	711.93	474.62	143	4.54
MF50	382.5	76.5	51	716.17	593.28	593.28	143	4.54
MF60	382.5	76.5	51	716.17	474.62	711.93	143	4.54
MF70	382.5	76.5	51	716.17	355.96	830.59	143	4.54
MF80	382.5	76.5	51	716.17	237.31	949.24	143	4.54
MF90	382.5	76.5	51	716.17	118.65	1067.90	143	4.54
MF100	382.5	76.5	51	716.17	0.00	1186.56	143	4.54

weighed initially before testing them under compression, and the final weight was taken after alternate wet and dry curing. The mass loss in the concrete specimen was determined. The compressive strength of the concrete cube specimens after alternate wet and dry test was determined.

3.2.2. Acid Test. Acid test was conducted on the concrete cubes of standard size of 100 mm × 100 mm × 100 mm to determine the residual compressive strength of the concrete cube specimens subjected to the acid exposure. The acid solution was prepared with 5% concentrated sulphuric acid diluted in one litre of water and filled in the container of needed quantity to use for all the different concrete mixes. The initial weight of the concrete specimen was taken, and then the specimen was immersed in the prepared diluted sulphuric acid solution. The *pH* of the acid solution was kept constant at 5 throughout the testing period by regularly replacing the acid solution for every period of 14 days. After immersion in sulphuric acid solution for periods of 56 days, 90 days, 120 days, 180 days, and 270 days, the concrete specimens of all kinds of the concrete mix were taken out. The concrete specimens were dried at room temperature for one hour to eliminate the surface moisture on the concrete surface. The concrete specimens after the acid exposure were exposed to compression with a digital compression testing machine of 1000 kN capacity. The acid test setup is shown in Figure 1.

3.2.3. Sulphate Test. A sulphate test was performed on the concrete cubes of standard size 100 mm × 100 mm × 100 mm to determine the residual compressive strength of the concrete mixes after the cubes were exposed to sulphate attack. The sulphate solution was set by dissolving 30000 mg of sodium sulphate in one litre of water and prepared for the immersion of the concrete specimens. The initial weight of each concrete specimen was taken and then the concrete specimen was immersed in the prepared sulphate solution. Spent-up sulphate solution was replaced with freshly prepared sulphate solution for every term of 14 days to keep the concentration of the solution constant throughout the testing period. The concrete specimens of all mix proportions adopted in the study were tested at ages of 56 days, 90 days, 120 days, 180 days, and 270 days. The final weight of the concrete specimens after acquaintance with sulphate attack was noted, and the loss in mass of the concrete specimen was calculated as the difference in initial and final weights of the concrete specimen. The concrete specimens were air-dried at room temperature for one hour to remove the saturated concrete surface and tested by using a digital compressive strength testing machine to determine the strength of concrete under compression affected by sulphate. The test setup for the sulphate test is shown in Figure 2.

Figure 1: Acid test setup.

3.3. Scanning Electron Microscope Analysis of Concrete. Break surface inspection was made at a smaller scale level through a scanning electron microscope (SEM) with a resolution of 50 to 100 nm and magnification up to 2 μm. SEM images are taken for the samples taken under compressive loads to identify spatial variation in the material properties of the object.

Figure 2: Sulphate test setup.

4. Proposed Strength Prediction Model

Concrete strength can be accurately predicted using response surface methodology (RSM). The quantities of cement, aggregates, water, and additives in the mix, as well as the curing conditions, all affect the strength of concrete. To comprehend and maximise these aspects and obtain the desired concrete strength, RSM offers an organised technique. A sequence of experiments is carried out by altering the relevant elements within a predetermined range in order to apply RSM to forecast the concrete strength. The ratios of natural aggregates, ferro slag, and curing age are among these variables. The concrete samples created in each experiment are then tested for strength. In order to create a mathematical model that explains the connection between the input variables and the concrete strength, the obtained data are statistically analysed. Either a regression model or a polynomial equation can be used to express the model. Each factor and its interactions' importance can be ascertained using RSM procedures like analysis of variance (ANOVA) [29]. The strength of concrete can be predicted using the mathematical model once it has been established for any given set of input variables falling within the experimental range. Additionally, the RSM optimisation technique is used to identify the ideal factor concentrations that produce the desired concrete strength. To determine the link between independent and outcome variables in RSM, the central composite design is used [30]. Equation (1) is then used to determine the ideal number of experiments.

$$N = 2^k + 2k + n, \tag{1}$$

where k = number of influences and n = number of center points [31]. To obtain the optimum outcomes, a quadratic model as shown in equation (2) was used.

$$Y = A_0 + \sum_{i-1}^{n} Aix_i + \sum_{i=1}^{n} A_{ii}x_i^2 + \sum_{i-1}^{n}\sum_{i=n}^{n} A_{ij}x_i x_j;\ (i \neq j), \tag{2}$$

where Y = response, A_0 = constant; A_i = linear coefficient, A_{ii} = quadratic coefficient, and A_{ij} = interactive coefficient.

Table 4: Compressive strength of different mix proportions.

Mix ID	Compressive strength (MPa)		
	3rd day	7th day	28th day
MF0	40.48	51.40	64.25
MF10	41.90	53.20	66.50
MF20	43.79	55.60	69.50
MF30	44.86	56.96	71.20
MF40	44.42	56.40	70.50
MF50	40.80	51.81	64.76
MF60	39.82	50.56	63.20
MF70	38.75	49.20	61.50
MF80	37.49	47.60	59.50
MF90	36.86	46.80	58.50
MF100	35.28	44.80	56.00

5. Results and Discussion

5.1. Optimum Concrete Mix. The compressive strength of the concrete cube specimens of all mix proportions was found at the age of 3 days, 7 days, and 28 days. It was detected from the experimental results that upsurge in the weight percentage of ferro slag aggregate increased the compressive strength of the concrete up to 40% substitution of natural aggregate and beyond this replacement level, the strength of the concrete mix began to reduce marginally compared to that of the strength of the reference/controlled concrete mix. The rise in the strength of the concrete was mainly due to the strong binding behavior of the ferro slag aggregate with natural aggregate, and this aspect holds good up to 40% replacement. It was believed that the adding fly ash and silica fume enhanced the strength properties of the concrete mix. From Table 4, three kinds of mixes–MF20, MF30, and MF40, having 20%, 30%, and 40% replacement by ferro slag aggregate, possessed higher compressive strengths of 69.50 MPa, 71.20 MPa, and 70.50 MPa, respectively, as compared to that of the strengths of all other mixes. The plain natural aggregate concrete shows significant compressive strength of 64.25 MPa. Hence, the optimised concrete mixes of MF20, MF30, and MF40 were chosen for further experimental studies. The particulars of the mix proportions with respect to reference the concrete mix and the optimised concrete mixes are displayed in Table 5.

5.2. Scanning Electron Microscope Analysis of Concrete. Scanning electron microscopy is a useful means to study the internal structure, chemical composition, size, shape, orientation, and binding of particles in concrete mixes [31]. Specimens of modified ferro slag aggregate concrete (MF30) prepared with 30% substitution of natural coarse aggregate by ferro slag aggregate and with the addition of silica fume and fly ash were examined under a scanning electron microscope. Images at 2.5 kx, 5 kx, 7 kx, 25 kx, and 50 kx magnifications were captured and studied, as shown in Figures 3 and 4.

Silica fume and fly ash chemically react with (Ca $(OH)_2$) leading to the creation of an additional C-S-H gel, which in turn increases the strength of concrete. Due to the

Table 5: Optimised mix proportion.

Mix ID	Cement	Fly ash	Silica fume	Coarse aggregates		Water	Superplasticizer
				Natural aggregates	Ferro slag aggregates		
			(kg/m^3)				(l/m^3)
MF0	382.5	76.5	51	1186.5	0	143	4.589
MF20	382.5	76.5	51	949.24	237.51	143	4.589
MF30	382.5	76.5	51	830.59	355.96	143	4.589
MF40	382.5	76.5	51	711.94	474.62	143	4.589

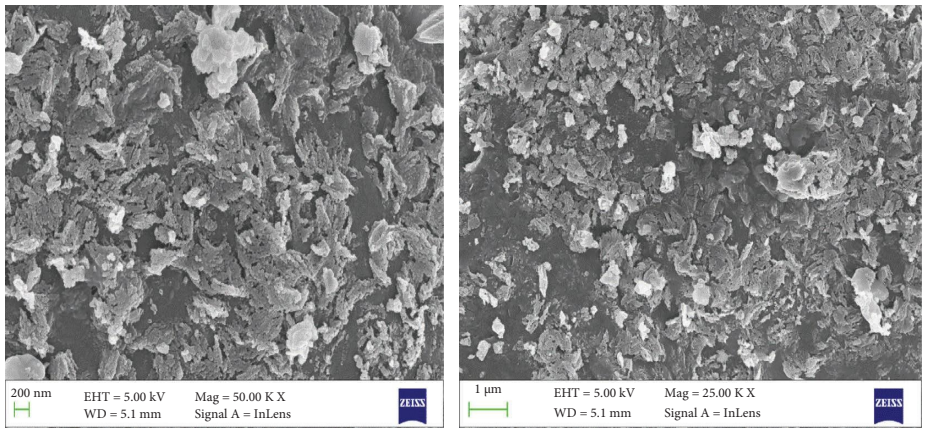

Figure 3: Scanning electron microscopic (SEM) images of modified ferro slag concrete at 25 kx and 50 kx magnifications.

substitution of cement with fly ash, the distribution of C-S-H decreased after 28 days of curing. In the mix, due to unreacted particles present, the development of C-S-H was less. Crystal deposition in the mixture's microstructure is minimal and other prominent mineral components include Ca $(OH)_2$ and calcite ($CaCO_3$). The strength decreases as a result of the lack of hydration of the cement paste's particles. The primary cause of this mixture's strength is the formation of an extra C-S-H gel as a result of the chemical reaction between silica fume and fly ash and Ca $(OH)_2$.

The SEM images of the modified ferro slag aggregate concrete illustrate the disposition of silica fume and fly ash particles and highlight the good bonding of these admixtures with the ferro slag aggregate. The mineral admixtures decrease the porosity and increase the density of the concrete. Fly ash occurs in the concrete matrix in the form of small hollow spherical particles. Silica fume is noticed in the form white solid ruptured particles. With its cementitious property, silica fume binds well with other ingredients and increases the impermeability of the concrete mix; also, it increases high strength and high density of the concrete. From the analysis of SEM images of the normal concrete mix and modified ferro slag concrete mix (MF30) captured at different resolutions, it is ascertained that the modified ferro slag concrete mix possesses better strength than the normal concrete mix.

5.3. Durability Tests. The concrete samples were exposed to various environmental conditions, and the durability attributes were assessed for a period of 270 days. The durability of the modified concrete mixes exposed to aggressive chemical environments was assessed through alternate wet and dry test, acid test, and sulphate test.

5.3.1. Alternate Wet and Dry Testing. The weights of concrete cube specimens of size 100 mm × 100 mm × 100 mm of normal concrete mix as well as modified concrete mix were taken, and then the concrete specimens were immersed in water with sodium chloride ($NaCl_2$) of 5 N for periods of 56 days, 90 days, 180 days, and 270 days. The specimens of concrete were removed, dried, and weighed. The concrete sample' compressive strength was assessed. The development of initial cracks was noticed in the concrete samples, irrespective of the mix proportions [32]. However, the cracks in the normal concrete specimen were wider than those observed in the concrete specimens of the modified concrete mixes. The observed results indicated that the compressive strength of the concrete specimen with ferro slag aggregate had shown improvement in the strength of the concrete compared to that of the plain nominal aggregate concrete for all mix proportions adopted. The percentage loss in compressive strength is shown in Table 6, and the compressive strength of concrete specimens after the wet and dry

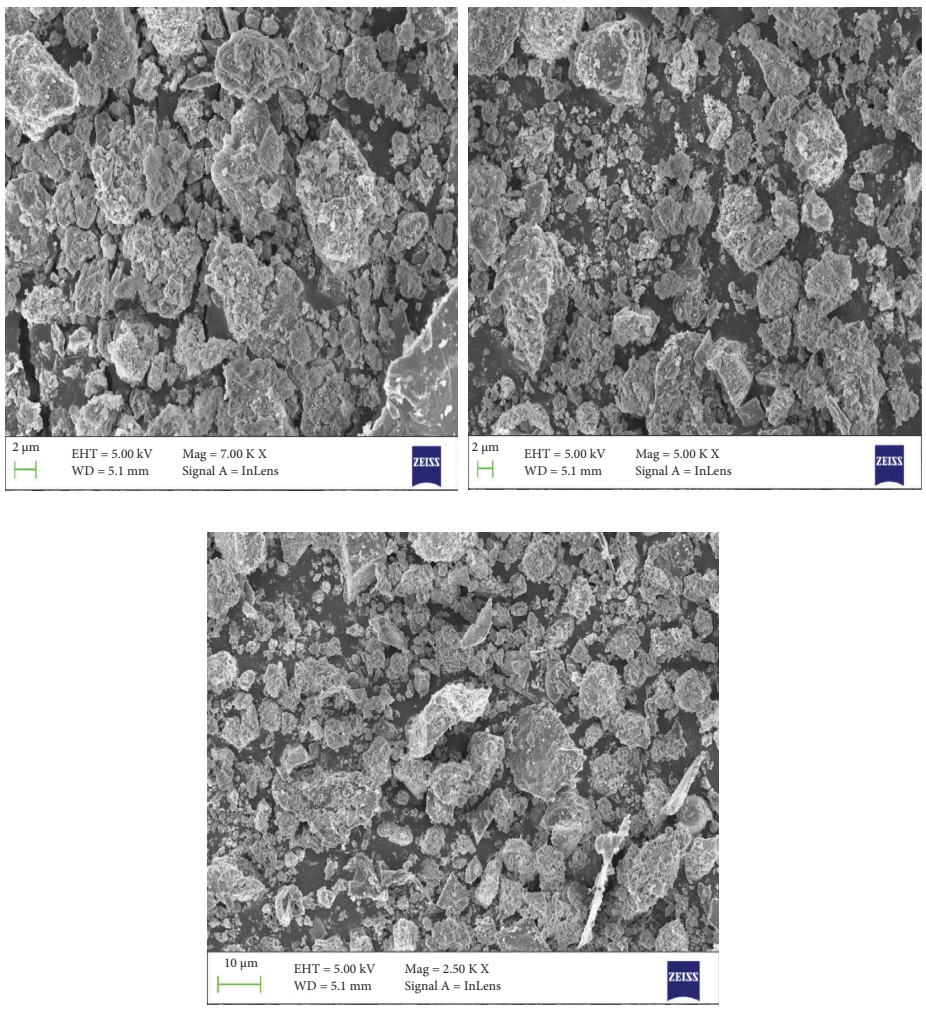

Figure 4: Scanning electron microscopic (SEM) images of modified ferro slag concrete at 7 kx, 5 kx, and 2.5 kx magnifications.

Table 6: Percentage loss in compressive strength after the wet and dry test.

Percentage loss in compressive strength due to wet and dry test				
Days	MF0	MF20	MF30	MF40
0 day	0	0	0	0
28 days	0.389	0.7194	1.685	2.127
56 days	3.346	1.438	3.792	4.255
90 days	6.303	2.733	6.601	7.801
180 days	11.284	6.474	10.814	9.929
270 days	15.953	13.669	12.921	14.893

processes is shown in Figure 5. From Figure 5, 30% replacement of the ferro slag showed higher compressive strength for 0, 28, 56, and 270 days. Similarly, from Table 7, it is found that percentage loss of weight due to alternate wetting and drying processes is minimum compared to conventional concrete irrespective of the number of days.

5.3.2. Acid Test. Compressive strength examinations on concrete cube specimens are used to evaluate the compressive strength of both the control concrete mix and the modified concrete mix. All of the concrete specimens were initially cured in water for twenty-eight days. The concrete specimens are then submerged for periods of 28 days, 56 days, 90 days, 180 days, and 270 days in an acidic solution of sulphuric acid of 1 N normalcy. After being exposed to chemical attack, the concrete specimens were removed, cleaned, and tested for compressive strength using a compression testing equipment of 2000 kN. Throughout the whole testing procedure, the loading rate was held constant at 2.5 kN/sec [33]. Table 8 and Figure 6 show the test results of the compressive strength of conventional and modified concrete mix after exposure to varying periods of acid environment. It was found that the concrete specimens of all the modified mixes evinced better compressive strength values than that of the normal concrete mix. Substitution of coarse aggregate up to 30% by ferro slag aggregate in the modified mixes produced the gradual increase in the compressive strength of the mixes; above 30% replacement, as in the case of mix MF40, the compressive strength got decreased. Silica fume and fly ash were added as admixtures to improve the density of the concrete mixes. The silica and pozzolanic material present in the admixtures imparted a stiff resistance to the concrete mixes against acid attack [10]. It was observed that the loss

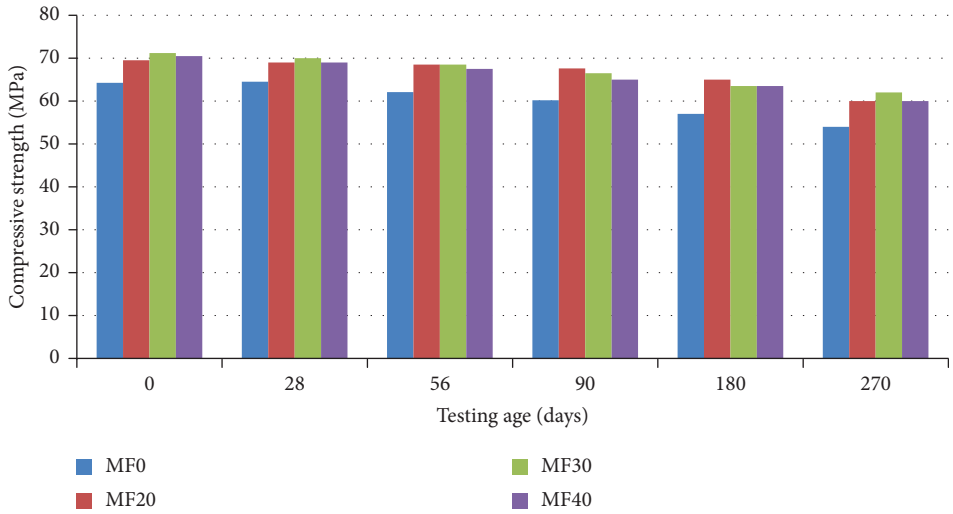

Figure 5: Compressive strength due to alternate wet and dry tests.

Table 7: Weight loss of specimens subjected to alternate wet and dry test.

Mix ID			*MF0*			
Days	0	28	56	90	180	270
Loss in %	1.21	4.06	6.50	8.13	9.34	10.56
Mix ID			*MF20*			
Days	0	28	56	90	180	270
Loss in %	0.00	2.00	5.61	7.22	8.42	9.61
Mix ID			*MF30*			
Days	0	28	56	90	180	270
Loss in %	0.39	1.58	3.16	4.34	5.53	7.11
Mix ID			*MF40*			
Days	0	28	56	90	180	270
Loss in %	0.38	3.10	5.03	6.20	7.75	8.91

Table 8: Loss in compressive strength due to acid attack.

Percentage loss in compressive strength due to acid attack				
Days	MF0	MF20	MF30	MF40
0 day	0.00	0.00	0.00	0.00
28 days	1.56	1.44	1.40	1.42
56 days	4.28	4.17	2.74	4.96
90 days	7.24	6.19	5.20	8.92
180 days	14.09	11.94	8.15	12.06
270 days	18.13	15.11	12.22	14.61

of weight due to acid attack was higher with respect to that of the reference mix (normal concrete mix with no replacement of natural aggregate) and was lower in the case of mix MF30 (modified concrete mix prepared with 30% replacement of natural aggregate by ferro slag aggregate). The decomposition and degradation of strength is due to the formation of hydration products when acids attack calcium hydroxide. The data on the loss of weight in specimens appear in Table 9.

5.3.3. Sulphate Test. Normative concrete mix and adapted concrete mix concrete cube samples were submerged in sulphate solution for various lengths of time, including 28 days, 56 days, 90 days, and 180 days. The concrete samples were removed after the sulphate assault phase, cleaned, and tested for compressive strength using a compressive strength testing machine. The residual compressive strength of the concrete that had been exposed to sulphate attack for various time periods and the weight loss of the concrete were two distinct metrics that were calculated. The experimental results revealed that after sulphate attack, the concrete specimens of modified concrete mix possessed higher residual compressive strength than that of the sulphate impregnated normal concrete mix [34]. The mineral admixtures silica fume and fly ash significantly improved the strength of both kinds of concrete mixes, i.e., normal concrete mix and adapted concrete mixes. It was surmised that the ferro slag, silica fume [35], and fly ash concrete combined very well with the ingredients of the concrete mix, increased the density of the concrete, and attributed to the high resistance of the specimens to sulphate attack [36]. The results of the sulphate attack test are shown in Table 10 and Figure 7.

It was observed from Table 11 that the weight loss of the concrete specimens of normal concrete mix with natural coarse aggregate was much higher than that of the modified concrete mix specimens prepared with partial addition of natural coarse aggregate by ferro slag aggregate. The weight loss due to the sulphate attack in the modified concrete mix specimens was much less because of the good binding of ferro slag aggregate with cement and sand and the consequent formation of a dense concrete matrix [37, 38].

5.4. RSM Model. In this study, response surface methodology-central composite design (CCD) is used to recognize the impact of independent parameters of natural

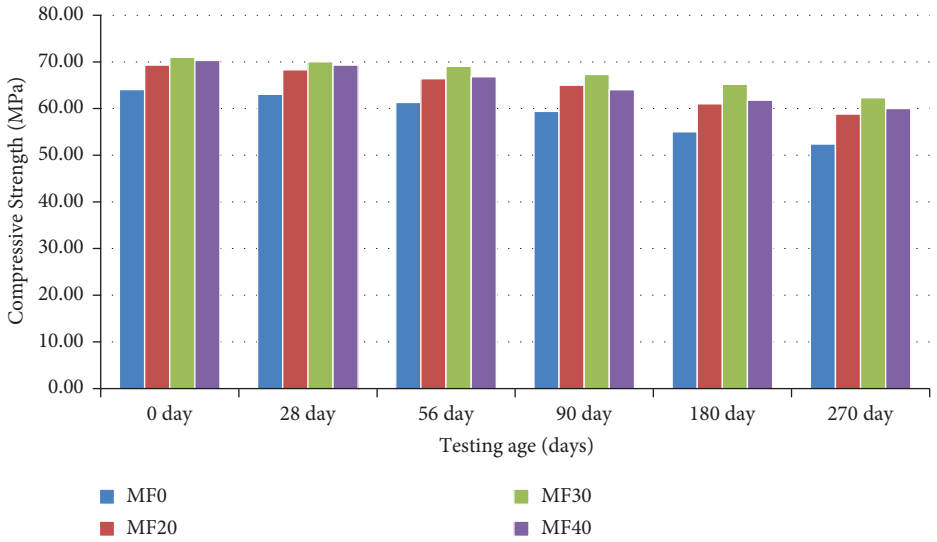

Figure 6: Compressive strength of conventional and modified concrete mixes.

Table 9: Weight loss of concrete mixes exposed to acid attack.

Mix ID			*MF0*			
Days	0	28	56	90	180	270
Loss in %	0.00	2.45	6.12	8.16	12.24	14.29
Mix ID			*MF20*			
Days	0	28	56	90	180	270
Loss in %	0.00	2.38	4.37	5.56	8.33	10.71
Mix ID			*MF30*			
Days	0	28	56	90	180	270
Loss in %	0.00	1.16	3.49	5.04	7.36	8.53
Mix ID			*MF40*			
Days	0	28	56	90	180	270
Loss in %	0.00	1.92	3.45	6.51	8.81	9.96

Table 10: Results of the compressive strength test on concrete mixes subjected to sulphate attack.

	Percentage loss in compressive strength due to sulphate attack			
Days	MF0	MF20	MF30	MF40
0 day	0.00	0.00	0.00	0.00
28 days	1.17	0.72	0.28	0.00
56 days	4.28	1.44	2.39	1.42
90 days	6.30	3.60	3.79	4.14
180 days	8.79	5.53	5.20	5.65
270 days	10.97	7.19	6.60	7.32

aggregate, ferro slag, and period of curing on the strength properties of concrete under wetting drying test, acid test, and sulphate attack. Based on test results obtained, a simplified model is proposed using regression analysis as shown in equations (3)–(5) for predicting the compressive strength of high-performance concrete. Natural aggregate, ferro slag, and curing period were considered basic variables for establishing the model.

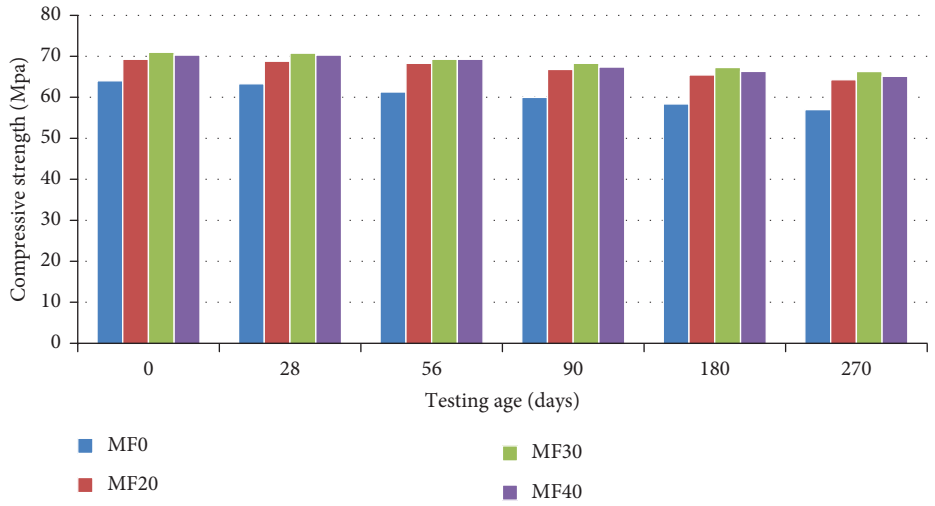

Figure 7: Compressive strength of different concrete mixes after sulphate attack.

Table 11: Loss of weight in concrete specimens exposed to sulphate attack.

Mix ID			*MF0*			
Period of exposure in days	0	28	56	90	180	270
Loss in %	0.39	3.57	6.34	8.33	12.30	14.68
Mix ID			*MF20*			
Period of exposure in days	0	28	56	90	180	270
Loss in %	0	1.91	5.36	8.04	10.3	11.87
Mix ID			*MF30*			
Period of exposure in days	0	28	56	90	180	270
Loss in %	0	1.13	3.01	7.19	8.71	9.84
Mix ID			*MF40*			
Period of exposure in days	0	28	56	90	180	270
Loss in %	0	1.91	3.83	8.81	9.57	11.11

Table 12: Analysis of variance (ANOVA) of CS_{WD}.

Source	DF	*F* value	*P* value
Model	9	1.26	0.362
Linear	3	1.91	0.192
NA	1	5.45	0.004
FS	1	0.16	0.697
CD	1	0.13	0.727
Square	3	0.95	0.455
NA^2	1	0.40	0.543
FS^2	1	1.12	0.315
CD^2	1	1.80	0.209
2-way interaction	3	0.91	0.469
NA ∗ FS	1	1.49	0.250
NA ∗ CD	1	0.54	0.481
FS ∗ CD	1	0.71	0.418
Error	10	0	0
Lack of fit	5	15.63	0.005

Table 13: Analysis of variance (ANOVA) of CS_{AT}.

Source	DF	*F* value	*P* value
Model	9	3.86	0.023
Linear	3	6.29	0.011
NA	1	6.69	0.027
FS	1	1.27	0.285
CD	1	10.90	0.003
Square	3	2.49	0.120
NA^2	1	2.67	0.134
FS^2	1	0.82	0.387
CD^2	1	3.34	0.098
2-way interaction	3	2.81	0.094
NA ∗ FS	1	1.79	0.211
NA ∗ CD	1	6.51	0.029
FS ∗ CD	1	0.13	0.723
Error	10	0	0
Lack of fit	5	1.23	0.413

Table 14: Analysis of variance (ANOVA) of CS_{ST}.

Source	DF	*F* value	*P* value
Model	9	3.56	0.030
Linear	3	6.31	0.011
NA	1	3.57	0.088
FS	1	1.43	0.259
CD	1	13.94	0.004
Square	3	4.23	0.036
NA^2	1	12.41	0.004
FS^2	1	0.53	0.484
CD^2	1	0.00	0.978
2-way interaction	3	0.15	0.928
NA ∗ FS	1	0.01	0.928
NA ∗ CD	1	0.02	0.881
FS ∗ CD	1	0.42	0.534
Error	10	0	0
Lack of fit	5	2.98	0.128

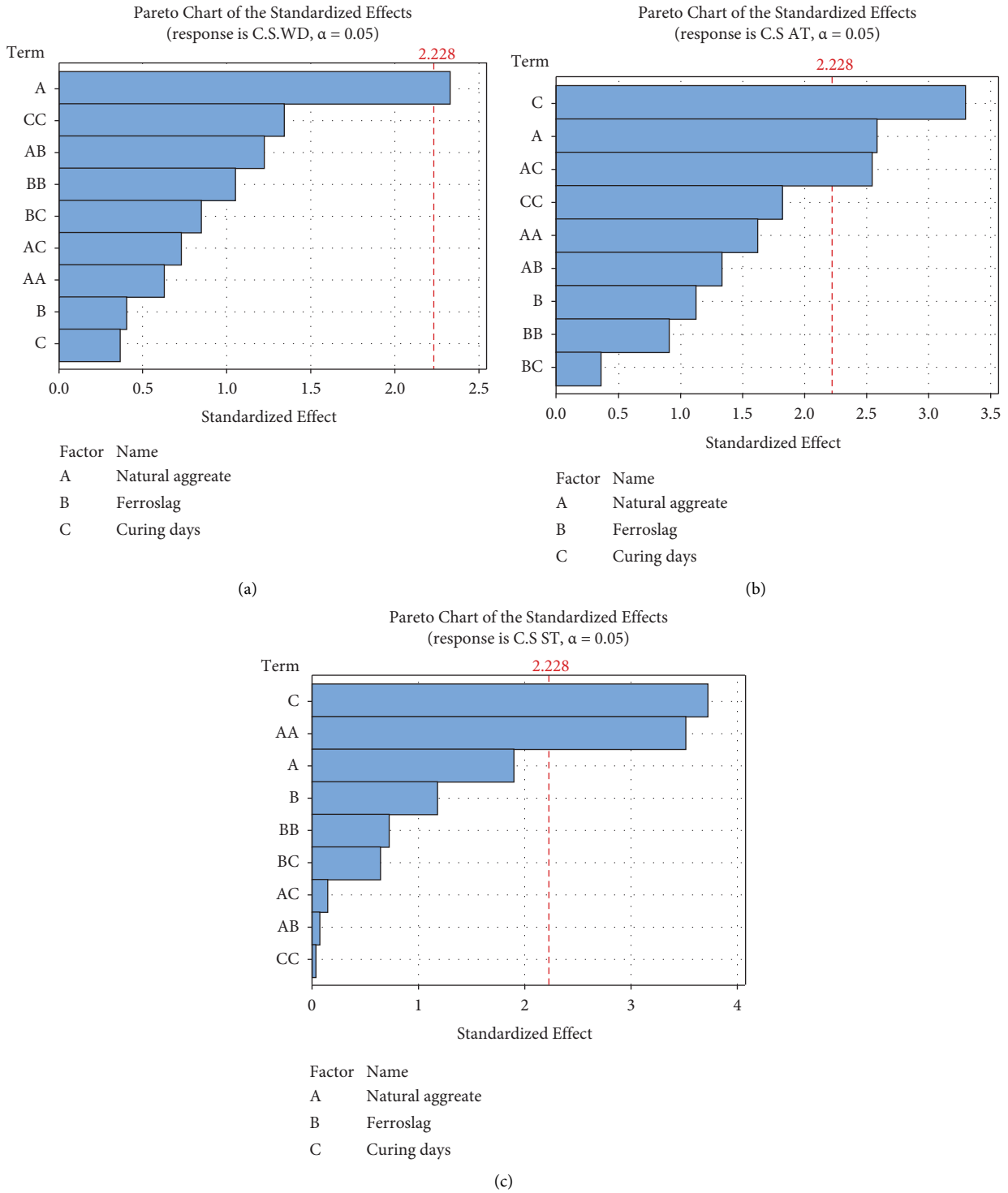

Figure 8: Pareto chart for (a) $\mathbf{CS_{WD}}$, (b) $\mathbf{CS_{AT}}$, and (c) $\mathbf{CS_{ST}}$.

Table 15: Percentage contribution of NA, FS, and CD.

Parameter	CS_{WD}	CS_{AT}	CS_{ST}
NA	42	38	21
FS	28	11	17
CD	30	51	62

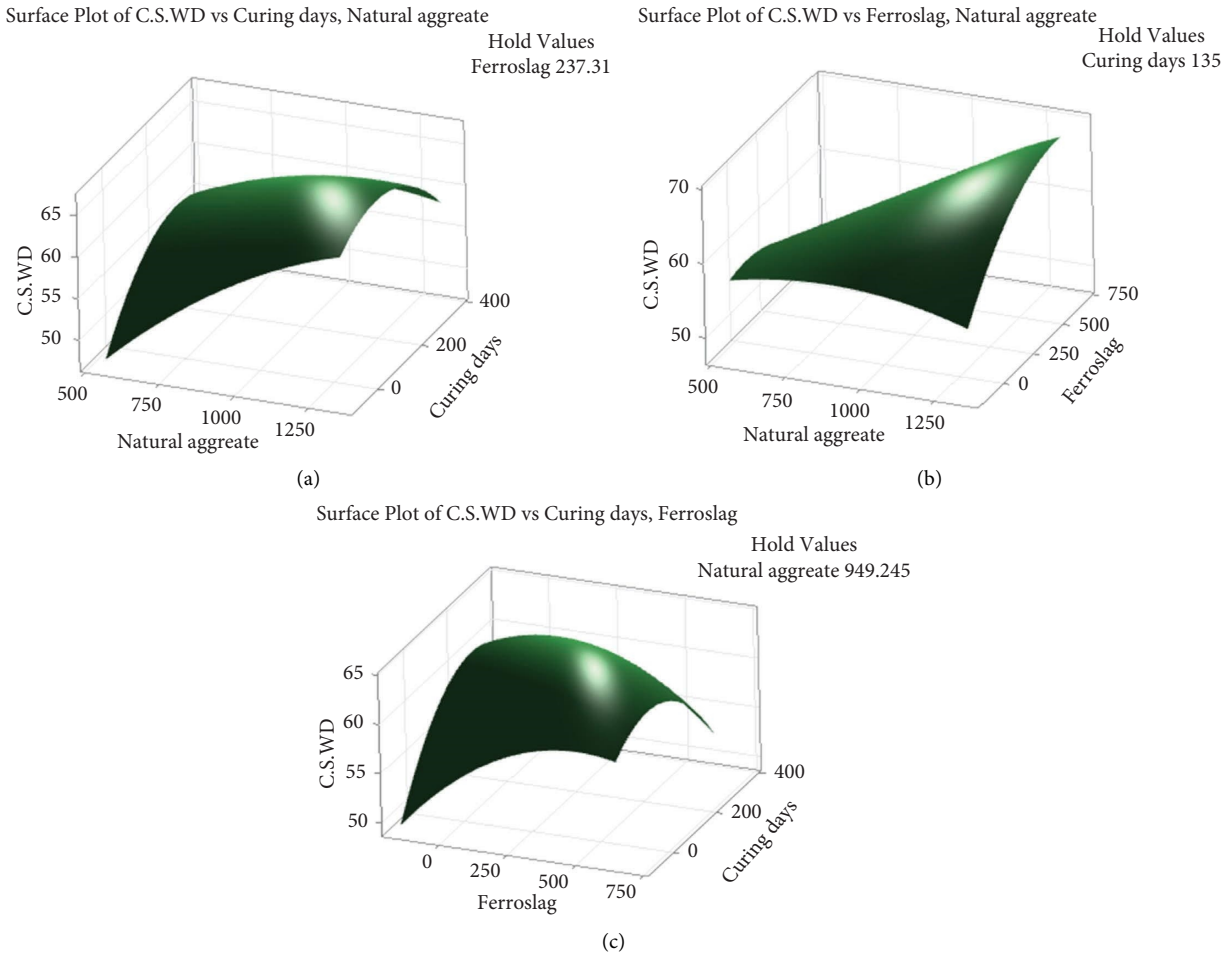

FIGURE 9: Surface plot for $\mathbf{CS_{WD}}$. (a) Curing days and natural aggregate. (b) Ferroslag and natural aggregate. (c) Curing days and ferroslag.

$$\begin{aligned} CS_{WD} = {} & 37.0 + 0.03NA - 0.0151FS + 0.0746CD - 0.000014\,(NA)^2 \\ & - 0.000023\,(FS)^2 - 0.000091\,(CD)^2 \\ & + 0.000036NA * FS - 0.000038NA * CD - 0.000044FS * CD, \end{aligned} \tag{3}$$

$$\begin{aligned} CS_{AT} = {} & 16.60 + 0.0676NA + 0.01201FS + 0.0735CD \\ & - 0.000022\,(NA)^2 + 0.000012\,(FS)^2 + 0.000077\,(CD)^2 \\ & - 0.000024NA * FS - 0.000082NA * CD + 0.000012FS * CD, \end{aligned} \tag{4}$$

$$\begin{aligned} CS_{ST} = {} & 30.0 + 0.0842NA + 0.0042FS - 0.0215CD - 0.000047\,(NA)^2 \\ & - 0.000010\,(FS)^2 - 0.000001\,(CD)^2 \\ & + 0.000002NA * FS - 0.00005NA * CD + 0.000020FS * CD, \end{aligned} \tag{5}$$

where CS_{WD}, CS_{AT}, and CS_{ST} represent the compressive strength of concrete under wetting drying test, acid test, and sulphate test, respectively. NA is natural aggregate, *FS* is ferro slag, and *CD* is the period of curing.

5.4.1. Lack of Fit (P Value) and Pareto Analysis. If the progression variable's respective p values are <0.005 and <0.001, then the progression variable is significant. If the p value of the progression variable is >0.005, it is considered

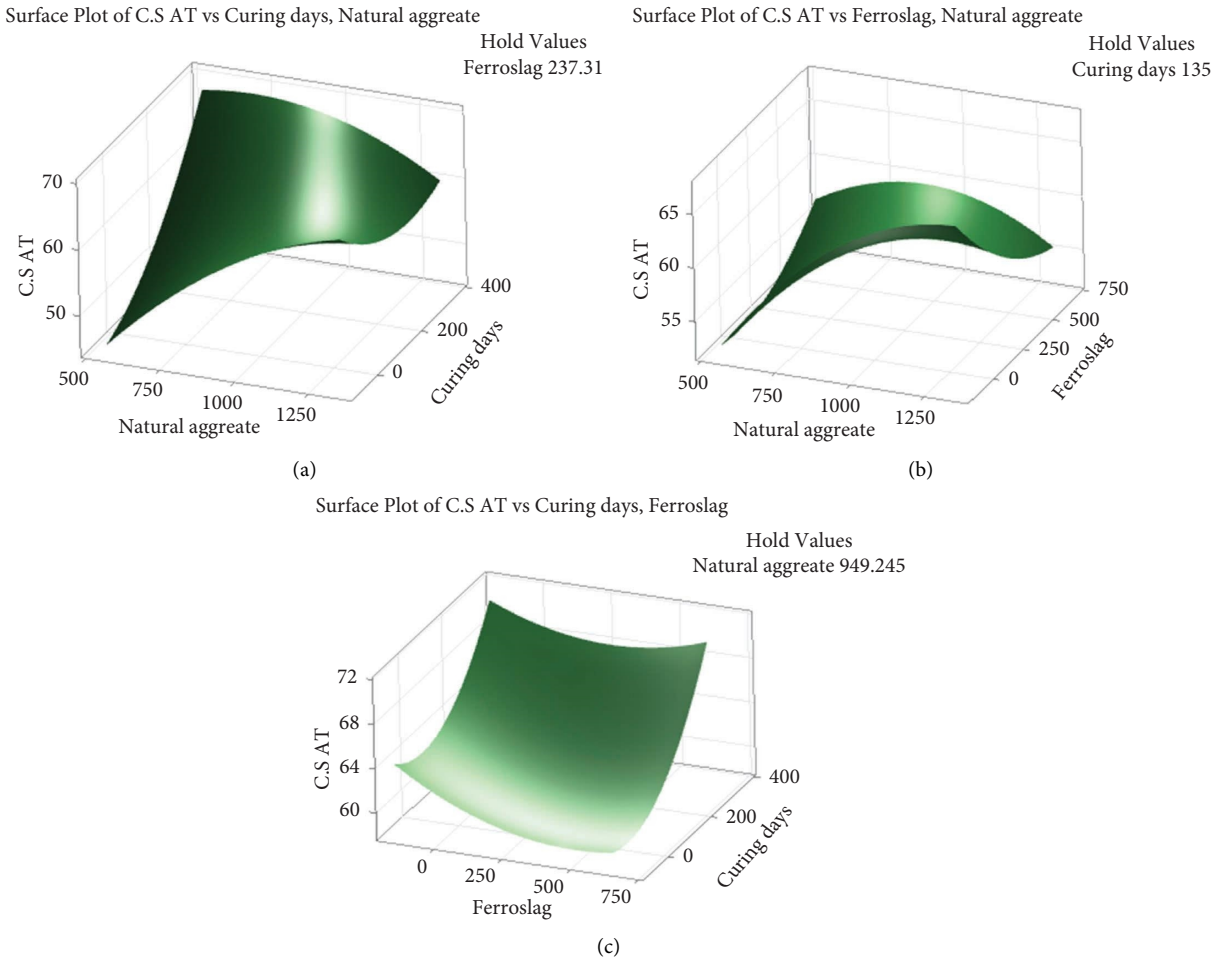

FIGURE 10: Surface plot for $\mathbf{CS_{AT}}$. (a) Curing days and natural aggregate. (b) Ferroslag and natural aggregate. (c) Curing days and ferroslag.

trivial. From ANOVA Table 12 the p value of NA is < 0.005 that clearly shows that they are significant in CSWD. Similarly from Table 13 it is seen that the p values of NA, CD, and NA $*$ CD are less than 0.005, which clearly indicates that linear NA, CD, and quadratic NA $*$ CD have significance in CS_{AT}. From Table 14, the value of p is less than 0.005 for linear CD and quadratic NA, which denotes that CD and NA have more significance in CS_{ST} compared to linear NA and FS.

Conferring to the Pareto chart in Figure 8, Linear (A) had a higher value than Linear (B and C), indicating that natural aggregate is more important than ferro slag and curing period for CS_{WD}. The F value of linear NA is higher in ANOVA (Table 12) compared to FS and CD, which provides further evidence that natural aggregates are considered a more significant factor in determining CS_{WD}. From Figure 8(b), the value of linear A and C and quadratic AC are more significant for CS_{AT}. Similar observations are made in Table 13 where the F value of linear NA, CD, and quadratic NA $*$ CD is high, which clearly indicates that natural aggregate and curing period contribute to CS_{AT}. From Figure 8(c), linear C and quadratic AA are higher than the standard value of 2.28 indicating that they are more significant in CS_{ST}. Similar results are found in Table 14 as the F values of linear CD and quadratic NA^2 are high. From the responses of CS_{WD}, CS_{AT}, and CS_{ST} it is apparent that the natural aggregate and curing period are the most significant factors which influence the compressive strength.

5.4.2. Surface Plot Analysis. In Figures 9–11, three-dimensional (3D) surface plots are displayed to show how progression variables affect the responses. From Figure 9, it is evident that concrete with 830.59 kg/m^3 of natural aggregate (70% by weight of concrete) and 355.96 kg/m^3 of ferro slag (30% by weight of concrete) after 135 days of curing under wet and dry, acid curing, and sulphate curing has the highest compressive strength. Although addition of ferro slag has increased the compressive strength under different curing conditions, their addition beyond 30% substitution and 270 days of curing the compressive strength decreased under wet and dry condition, acid test, and sulphate test. The influence of natural aggregate, ferro slag, and curing days on CS_{WD}, CS_{AT}, and CS_{ST} is shown in Table 15.

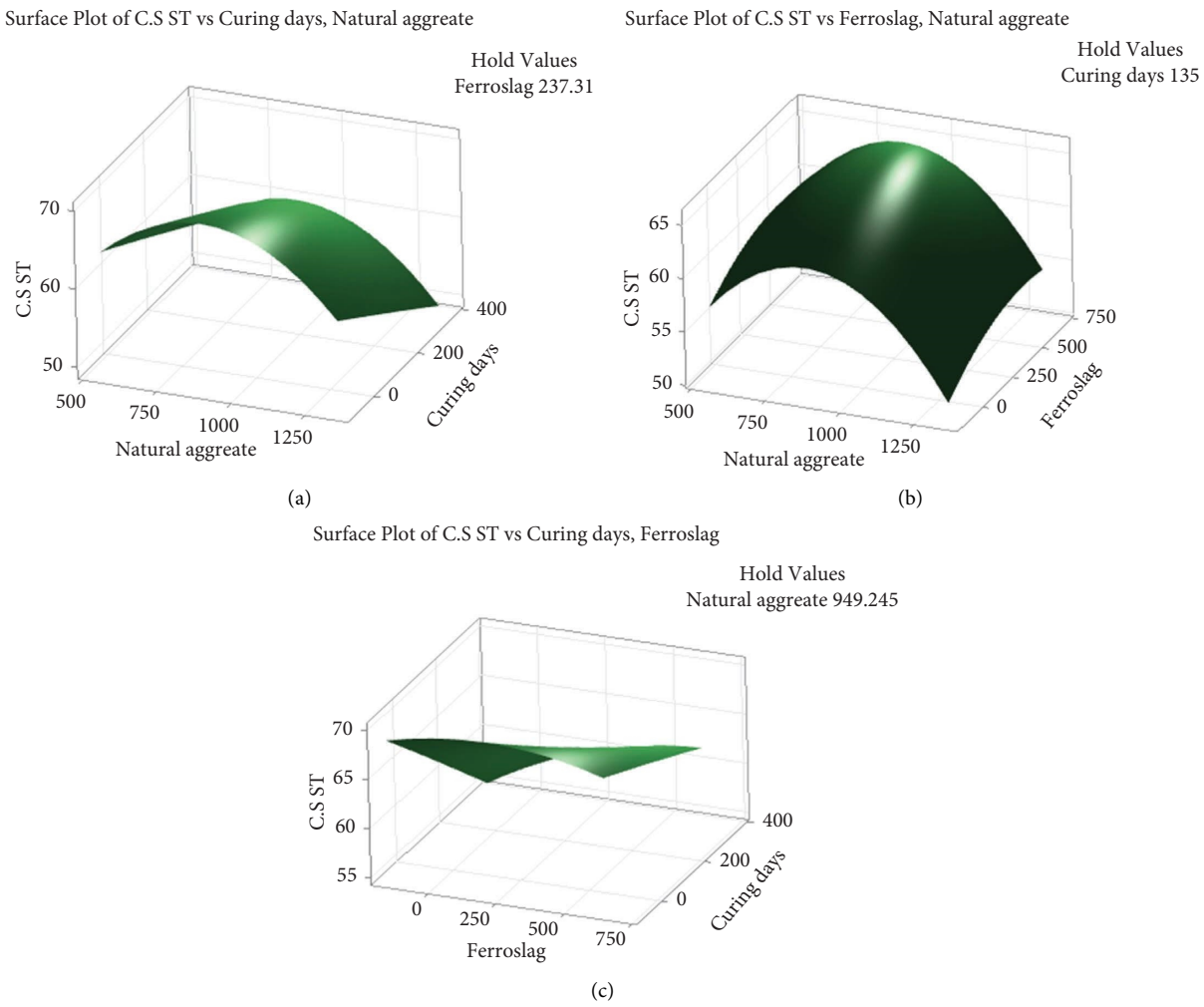

FIGURE 11: Surface plot for $\mathbf{CS_{ST}}$. (a) Curing days and natural aggregate. (b) Ferroslag and natural aggregate. (c) Curing days and ferroslag.

The contributions to the compressive strength due to alternate wetting and drying, acid test, and sulphate test due to the dosages of natural aggregate (1186.5 kg/m^3, 949.24 kg/m^3, 830.59 kg/m^3, and 711.94 kg/m^3) and ferro slag (0, 237.51 kg/m^3, 355.96 kg/m^3, and 474.62 kg/m^3) at curing ages of 0, 28, 56, 90, 180, and 270 days are shown in Table 15. As shown in the table, the contributions of the NA and FS and their interaction to the compressive strength of concrete varied widely depending on the curing age and curing regime. The effect of NA on CS_{WD} was 42% at 28 days and was reduced to 38% and 21% for CS_{AT} and CS_{ST}, respectively. On the other hand, the contribution of curing days was 30%, 51%, and 62% for CS_{WD}, CS_{AT}, and CS_{ST}, respectively. The percentage contribution of FS is very minimum when compared to other parameters.

6. Conclusions

To determine the combined effect of fly ash, silica fumes, and ferro slag aggregate on high-performance concrete, an experimental examination was conducted. Additionally, RSM was utilised to forecast the compressive strength of concrete in several tests, including wetting dry, acid, and sulphate. The important conclusions derived from the findings are listed below:

(i) The maximum compressive strength of 71.20 MPa is observed for 30% substitution of the ferro slag which is about 30% higher than conventional concrete.

(ii) The high compressive strength was due to the bonding of ferro slag aggregates with the cement, fly ash, and silica fume in the hydration process. High dense concrete was obtained due to the ferro slag aggregate.

(iii) The residual compressive strength under acid attack was higher for the ferro slag aggregate, and it was found to be 30% replacement of ferro slag as an optimum dosage for 270 days, 62.50 MPa compared to that of the conventional concrete of 52.60 MPa.

(iv) The weight loss of concrete under acid attack for 270 days period is 8.53% compared with 14.29% of conventional concrete.

(v) In chloride attack for 270-day period, the residual compressive strength of the concrete was higher for the 30% replacement of ferro slag with a value of 65.20 MPa compared to that of the conventional concrete of 55.60 MPa.

(vi) Similarly, sulphate and alternate wet and drying tests on the concrete also showed higher residual compressive strength of the concrete when associated with that of the conventional concrete.

(vii) According to the analysis of variance results, natural aggregate, ferro slag, and the curing duration were the main contributing factors for CS_{WD}, CS_{AT}, and CS_{ST}. The results of the ANOVA and Pareto chart analysis exhibited that the regression models for CS_{WD}, CS_{AT}, and CS_{ST} are quite significant.

(viii) Given that the models' p values were <0.005, their outputs are highly accurate. The natural aggregate, ferro slag, and curing period are the most important factors for CS_{WD}, CS_{AT}, and CS_{ST} according to the outcomes of regression analysis, Pareto chart, and surface plot analysis.

(ix) From this study, it was clear that the ferro slag aggregate can be used as coarse aggregate as a fractional substitution of natural coarse aggregate and the same was experimentally proved under different conditions. Thus, using ferro slag aggregates in the building sector will be a practical way to prevent the destruction of the environment.

Data Availability

The data used to support the findings of this study are available from the corresponding author upon request.

Conflicts of Interest

The authors declare that they have no conflicts of interest.

References

[1] B. H. Bharat Kumar, R. Narayanan, B. K. Raghu prasad, and D. Ramachandramurthy, "Mix proportioning of high-performance concrete," *Cement and Concrete Composites*, vol. 23, no. 1, pp. 71–80, 2001.

[2] J. J. Chen, P. Ng, L. Li, and A. Kwan, "Production of high-performance concrete by addition of fly ash microsphere and condensed silica fume," *Procedia Engineering*, vol. 172, pp. 165–171, 2017.

[3] C. Gu, W. Sun, L. Guo et al., "Investigation of microstructural damage in ultrahigh- Performance concrete under freezing – thawing action," *Advances in Materials Science and Engineering*, vol. 2018, Article ID 3701682, 9 pages, 2018.

[4] J. Liu and R. Guo, "Applications of steel slag powder and steel slag aggregate in ultra-high performance concrete," *Advances in Civil Engineering*, vol. 2018, Article ID 1426037, 8 pages, 2018.

[5] P. S. Kothai and R. Malathy, "Enhancement of concrete properties by steel slag as a partial replacement material for coarse aggregates," *Australian Journal of Basic and Applied Sciences*, vol. 7, no. 12, pp. 278–285, 2013.

[6] E. Mohseni, M. M. Ranjbar, and K. D. Tsavdaridis, "Durability properties of high-performance concrete incorporating Nano-Tio_2 and fly ash," *American Journal of Engineering and Applied Sciences*, vol. 8, no. 4, pp. 519–526, 2015.

[7] S. A. Tarawneh, E. S. Gharaibeh, and F. M. Saraireh, "Effect of using steel slag aggregate on mechanical properties of concrete," *American Journal of Applied Sciences*, vol. 11, no. 5, pp. 700–706, 2014.

[8] Y. Guo, J. Xie, W. Zheng, and J. Li, "Effects of steel slag as fine aggregate on static and impact behaviours of concrete," *Construction and Building Materials*, vol. 192, pp. 194–201, 2018.

[9] K. X. Zhuo, G. T. Liu, X. W. Lan et al., "Fracture Behavior of Steel Slag Powder-cement-based concrete with different steel-slag-powder replacement ratios," *Materials*, vol. 15, no. 6, pp. 2243–2315, 2022.

[10] P. Aïtcin, "The durability characteristics of high- performance concrete: a review," *Cement and Concrete Composites*, vol. 25, no. 4-5, pp. 409–420, 2003.

[11] S. K. Verma, S. S. Bhadauria, and S. Akhtar, "Monitoring corrosion of steel bars in reinforced concrete structures," *The Scientific World Journal*, vol. 2014, Article ID 957904, 9 pages, 2014.

[12] J. Sridhar, D. Jegatheeswaran, D. Vivek, and G. Elias, "Flexural behaviour of chicken mesh ferrocement laminates with partial replacement of fine aggregate by steel slag," *Advances in Materials Science and Engineering*, vol. 2021, Article ID 7307493, 9 pages, 2021.

[13] M. Soundararajan, S. Balaji, J. Sridhar, and G. Ravindran, "Sustainable retrofitting and moment evaluation of damaged RC beams using ferrocement composites for vulnerable structures," *Sustainability*, vol. 14, no. 15, pp. 9220–9316, 2022.

[14] C. S. Jerold Samuel and A. Ramesh, "Investigation on microstructure and tensile behaviour of stir cast LM13 Aluminium alloy reinforced with copper coated short steel fibres using response surface methodology," *Transactions of the Indian Institute of Metals*, vol. 71, no. 9, pp. 2221–2230, 2018.

[15] Y. Moodi, S. R. Mousavi, A. Ghavidel, M. R. Sohrabi, and M. Rashki, "Using response surface methodology and providing a modified model using whale algorithm for estimating the compressive strength of columns confined with FRP sheets," *Construction and Building Materials*, vol. 183, pp. 163–170, 2018.

[16] S. J. S. Chelladurai, R. Arthanari, A. N. Thangaraj, and H. Sekar, "Dry sliding wear characterization of squeeze cast LM13/FeCu composite using response surface methodology," *China Foundry*, vol. 14, no. 6, pp. 525–533, 2017.

[17] J. Sridhar, G. B. Shinde, D. Vivek et al., "Response surface methodology approach to predict the flexural moment of ferrocement composites with weld mesh and steel slag as partial replacement for fine aggregate," *Advances in Material science and Engineering*, vol. 2022, Article ID 9179480, 9 pages, 2022.

[18] A. Hammoudi, K. Moussaceb, C. Belebchouche, and F. Dahmoune, "Comparison of artificial neural network

(ANN) and response surface methodology (RSM) prediction in compressive strength of recycled concrete aggregates," *Construction and Building Materials*, vol. 209, pp. 425–436, 2019.

[19] A. Poorarbabi, M. Ghasemi, and M. M. Azhdary, "Concrete compressive strength prediction using non-destructive tests through response surface methodology," *Ain Shams Engineering Journal*, vol. 11, no. 4, pp. 939–949, 2020.

[20] Q. Sun, H. Zhu, H. Li, H. Zhu, and M. Aao, "Application of response surface methodology in the optimization of fly ash geopolymer concrete," *Romanian Journal of Materials*, vol. 48, no. 1, pp. 45–52, 2018.

[21] S. Ahmed, Z. Mahaini, F. Abed, M. A. Mannan, and M. Al-Samarai, "Microstructure and mechanical property evaluation of dune sand reactive powder concrete subjected to hot air curing," *Materials*, vol. 15, no. 1, pp. 41–18, 2021.

[22] Z. Zhu, X. Lian, X. Zhai, X. Li, M. Guan, and X. Wang, "Mechanical properties of ultra high- performance concrete with coal gasification coarse slag as river," *Sand Replacement" Materials*, vol. 15, no. 21, pp. 1–17, 2022.

[23] P. Smarzewski, "Fresh and Mechanical Properties of high-performance self-compacting concrete containing ground granulated blast furnace slag and polypropylene fibres," *Applied Sciences*, vol. 13, no. 3, pp. 1975–2017, 2023.

[24] Bureau of Indian Standards, *IS12269- Ordinary Portland Cement 53 Grade-Specification*, Bureau of Indian Standards, Manak Bhawan Old Delhi, Delhi, India, 2013.

[25] Bureau of Indian Standards, *IS 383- Specifications for Coarse and Fine Aggregate from Natural Source of concrete*, Manak Bhawan Old Delhi, Delhi, India, 2016.

[26] Aci Committee, "Guide for selecting properties for high-performance concrete with portland cement and fly ash," ACI manual of Concrete Practice, Poznań, Poland, ACI 211.4R.93, 2001.

[27] Bureau of Indian Standards, "Methods of tests for strength of concrete," Manak Bhawan Old Delhi, Delhi, India, Is: 516, 1959.

[28] Bureau of Indian Standards, *IS 4332: Part 4, Methods of Test for Stabilized Soils-Wetting and Drying, and Freezing and Thawing Tests for Compacted Soil-Cement Mixtures*, Bureau of Indian Standards, Delhi, India, 1968.

[29] Astm, *Standard Test Method for Length Change of Hardened Hydraulic-Cement Mortar and concrete*, ASTM, Conshohocken, PA, USA, 1994.

[30] W. Wang, Y. Cheng, and G. Tan, "Design Optimization of SBS-modified asphalt mixture reinforced with eco-friendly basalt fiber based on response surface methodology," *Materials*, vol. 11, no. 8, pp. 1311–1322, 2018.

[31] S. Arumugam, G. Sriram, and T. Rajmohan, "Multi-response optimization of epoxidation process parameters of rapeseed oil using response surface methodology (RSM)-based desirability analysis," *Arabian Journal for Science and Engineering*, vol. 39, no. 3, pp. 2277–2287, 2014.

[32] P. Kumar Mehta and P. J. M. Monteiro, *Concrete – Microstructure, Properties and Materials*, The McGraw – Hill, New York, NY, USA, 3rd edition, 2006.

[33] K. Hassan, J. Cabrera, and R. Maliehe, "The effect of mineral admixtures on the properties of high- performance concrete," *Cement and Concrete Composites*, vol. 22, no. 4, pp. 267–271, 2000.

[34] M. Verapathran and P. Murthi, "Acid resistance and rapid chloride permeability of high- performance concrete," *International Journal of Chemical Sciences*, vol. 14, no. 2, pp. 1016–1027, 2016.

[35] P. Tumidajski and G. Chan, "Effect of sulfate and carbon dioxide on chloride diffusivity," *Cement and Concrete Research*, vol. 26, no. 4, pp. 551–556, 1996.

[36] R. Duval, E. Kadri, and E. H. Kadir, "Influence of silica fume on the workability and the compressive strength of high-performance concretes-performance concrete," *Cement and Concrete Research*, vol. 28, no. 4, pp. 533–547, 1998.

[37] W. T. Kuo, C. C. Liu, and J. Y. Wang, "Evaluation of the sulfate resistance of fly ash and slag concrete by using modified ACMT," *Construction and Building Materials*, vol. 49, pp. 40–45, 2013.

[38] M. D. Cohen and B. Mather, "Sulphate attack on concrete-research needs," *ACI Materials Journal*, vol. 88, no. 1, pp. 43–47, 1991.